

---

# Contextual Bayesian optimization with binary outputs

---

Tristan Fauvel

Sorbonne Université, INSERM, CNRS, Institut de la Vision  
F-75012 Paris, France

Matthew Chalk

## Abstract

Bayesian optimization (BO) is an efficient method to optimize expensive black-box functions. It has been generalized to scenarios where objective function evaluations return stochastic binary feedback, such as success/failure in a given test, or preference between different parameter settings. In many real-world situations, the objective function can be evaluated in controlled ‘contexts’ or ‘environments’ that directly influence the observations. For example, one could directly alter the ‘difficulty’ of the test that is used to evaluate a system’s performance. With binary feedback, the context determines the information obtained from each observation. For example, if the test is too easy/hard, the system will always succeed/fail, yielding uninformative binary outputs. Here we combine ideas from Bayesian active learning and optimization to efficiently choose the best context and optimization parameter on each iteration. We demonstrate the performance of our algorithm and illustrate how it can be used to tackle a concrete application in visual psychophysics: efficiently improving patients’ vision via corrective lenses, using psychophysics measurements.

generalized to situations where one can only obtain the performance of the system in the form of a binary output, corresponding, for example, to whether the system passes/fails a test (Tesch et al., 2013). Examples of binary Bayesian optimization (BBO) include testing whether a robot is able to successfully maneuver across a given environment, or the optimization of a model’s hyperparameters, by early-stopping the training of under-performing models while continuing others (Zhang et al., 2019). In these cases, the way the system is tested is critical in optimizing its performance. For example, if we ask a robot to move across an impossibly complex environment (e.g. filled with obstacles and pot-holes), it will always fail, leaving us none the wiser as to how to improve its performance.

A similar problem arises in preferential Bayesian optimization (PBO), where the performance of a system is evaluated via a set of comparisons between different parameter settings (Brochu et al., 2010). For example, PBO was used to improve the performance of hearing aid devices, by asking patients to evaluate which of two parameter settings they preferred, when listening to excerpts of music (Nielsen et al., 2014). In this example, the context (i.e. the audio stimuli) clearly plays a role in determining how much information is gained from subjects’ responses: an audio stimulus that was overly simple (e.g. a single monotone pitch) or random (e.g. white noise) would result in non-informative responses from subjects, impeding progress in optimizing the hearing device for most daily settings.

Here we show how to extend previous BO algorithms to deal with these two related problems, in which the measured performance of a system takes the form of a binary, context-dependent, output. We then show how this problem can be efficiently solved by applying a simple heuristic, where BO is used to maximize the system’s performance, while Bayesian active learning is used to choose a new context, such that the observed binary output (e.g. whether the system passed/failed a given test, or a comparison between two parameter settings) is maximally informative about the system’s performance. We show that our resulting algorithm per-

## 1 Introduction

Bayesian optimization (BO) has been used in many applications to optimize systems whose performance is expensive to evaluate, such as a robot’s walking motion (Antonova et al., 2017), deep brain stimulation (Grado et al., 2018), or machine learning model hyperparameters (Snoek et al., 2012). BO has also been

forms competitively on a range of benchmark problems. Further, we illustrate the relevance of our algorithm by applying it to a real-world problem, where the goal is to find the correct optical correction required to optimize a patient’s vision, based on their binary responses in a psychophysics task.

## 2 Problem statement

Consider a system, whose performance can be quantified by a function,  $g(\mathbf{x})$ . For example,  $g(\mathbf{x})$  could represent the visual acuity (VA) of a patient fitted with glasses with optical parameters,  $\mathbf{x}$ . We are interested in solving the global optimization problem:

$$\mathbf{x}^* = \arg \max_{\mathbf{x} \in \mathcal{X}} g(\mathbf{x}), \quad (1)$$

where  $\mathcal{X}$  is a bounded set denoted as the search space.

We consider the case where the performance of the system cannot be evaluated directly, but instead, can be assessed by observing whether it passes/fails a test in a given context, parameterized by  $\mathbf{s}$ . For example, we could test whether a subject (fitted with glasses with optical parameters,  $\mathbf{x}$ ) can correctly identify a visual stimulus, parameterized by  $\mathbf{s}$ , presented onscreen. The outcome of such a test is denoted by a binary variable,  $c$ , with success probability given by:

$$p(c = 1 | \mathbf{x}, \mathbf{s}) = \Phi(f(\mathbf{s}, \mathbf{x})), \quad (2)$$

where  $\Phi$  is the normal cumulative distribution function, and  $f(\mathbf{s}, \mathbf{x})$  is a function describing performance of the system with parameters  $\mathbf{x}$  and given a context  $\mathbf{s}$ .

If we are to optimize the system based on observed binary outcomes,  $c$ , the probability that the system passes a test in a given context,  $\mathbf{s}$  (determined by  $f(\mathbf{s}, \mathbf{x})$ ) must be closely related to its overall performance,  $g(\mathbf{x})$ . For simplicity, we begin by assuming that the same configuration,  $\mathbf{x}^*$ , maximizes performance in all contexts, such that:

$$\forall \mathbf{s} \in \mathcal{S}, \quad \arg \max_{\mathbf{x} \in \mathcal{X}} g(\mathbf{x}) = \arg \max_{\mathbf{x} \in \mathcal{X}} f(\mathbf{s}, \mathbf{x}), \quad (3)$$

where  $\mathcal{S}$  is a bounded set denoted as the context space. In our previous example, this would imply that the optical correction that maximizes VA also maximizes the subject’s performance in identifying a range of different visual stimuli, parameterized by  $\mathbf{s}$ . This condition will be true for a broad range of situations in which  $f(\mathbf{s}, \mathbf{x})$  takes the form:

$$f(\mathbf{s}, \mathbf{x}) = q(h(\mathbf{s})g(\mathbf{x}) + b(\mathbf{s})) \quad (4)$$

where  $h(\mathbf{s})$  is non-negative for all  $\mathbf{s}$ , and  $q(\cdot)$  is a monotonically increasing one-dimensional function. Plugging this back into Eqn 2, we have:

$$p(c = 1 | \mathbf{s}, \mathbf{x}) = \Phi[q(h(\mathbf{s})g(\mathbf{x}) + b(\mathbf{s}))]. \quad (5)$$

We can think of  $b(\mathbf{s})$  and  $h(\mathbf{s})$  as controlling the difficulty of the test. Without loss of generality, we can assume that  $g(\mathbf{x}) \geq 0$  for all  $\mathbf{x}$ . For large  $h(\mathbf{s})$  the probability of success will saturate close to 1 for all  $\mathbf{x}$ : i.e., the task is easy, so the system always passes the test. In contrast, when  $h(\mathbf{s})$  is close to zero, the system will perform close to baseline, with success probability  $\Phi(q(b(\mathbf{s})))$ . In both these extreme cases, little information is gained about the parameters,  $\mathbf{x}$ , that optimize performance, since the success probability depends only weakly on  $g(\mathbf{x})$ . Our goal, therefore, is to find a sampling rule that selects  $(\mathbf{s}, \mathbf{x})$  on each trial so as to appropriately set the difficulty of the task, and efficiently optimize  $g(\mathbf{x})$  in a limited number of trials.

## 3 Contextual binary Bayesian optimization

### 3.1 Inference

As is standard in BO, we will build a surrogate model of  $f(\mathbf{s}, \mathbf{x})$ , by assuming a zero-mean Gaussian process (GP) prior, such that  $f \sim GP(0, k(\cdot, \cdot))$ , where  $k$  is a kernel function. When the observed outcome is binary, the posterior probability distribution over  $f$  cannot be written analytically but must be approximated. While a number of different approximations schemes exist, here we use the Laplace approximation, since it is standard and simple to implement (Rasmussen & Williams, 2006). However, our approach could be applied to other approximation schemes such as expectation propagation (Minka, 2001; Seeger, 2002).

Ideally, the kernel should reflect prior knowledge about the objective, such as the fact that the optimum does not depend on the context. This can be done, for example, by assuming a multiplicative structure of the function of the form  $f(\mathbf{s}, \mathbf{x}) = h(\mathbf{s})g(\mathbf{x})$ , which in practice can be incorporated by using a kernel that decomposes as:  $k(\mathbf{s}, \mathbf{x}, \mathbf{s}', \mathbf{x}') = k_1(\mathbf{s}, \mathbf{s}')k_2(\mathbf{x}, \mathbf{x}')$ . Moreover,  $h$  should be constrained to be positive. In practice, we did not use this latter constraint in our experiments, as this would make the inference more difficult and it did not seem to impede performance.

### 3.2 Knowledge gradient acquisition rule

Having inferred a Bayesian model of the objective function,  $p(f|\mathcal{D})$ , the next step of any BO algorithm is to select new parameters,  $\mathbf{x}$  and  $\mathbf{s}$ , to evaluate the objective. To do this, we extended the ‘knowledge gradient’ (KG) acquisition rule, developed previously for BO with continuous outputs (Frazier et al., 2009), to contextual BBO.

We first explain our binary KG algorithm for standard

BBO (i.e with no contextual variable,  $\mathbf{s}$ ). As in standard KG, the reported solution of the optimization routine at iteration  $t$  is assumed to be the maximum of the posterior mean of the GP after observing data  $\mathcal{D}_t = (\{\mathbf{x}_1, c_1\}, \{\mathbf{x}_2, c_2\}, \dots, \{\mathbf{x}_t, c_t\})$ , that is:

$$\mu_{\mathcal{D}_t}^* = \arg \max_{\mathbf{x} \in \mathcal{X}} \mathbb{E}[g(\mathbf{x}) | \mathcal{D}_t]. \quad (6)$$

The KG corresponds to the expected increase in  $\mu^*$  if we are allowed one additional observation,  $\{\mathbf{x}_{t+1}, c_{t+1}\}$ :

$$\text{KG}(\mathbf{x}_{t+1}) = \sum_{c_{t+1}=0,1} p(c_{t+1} | \mathbf{x}_{t+1}, \mathcal{D}_t) \mu_{\mathcal{D}_t, \mathbf{x}_{t+1}, c_{t+1}}^* - \mu_{\mathcal{D}_t}^* \quad (7)$$

where  $p(c_{t+1} = 1 | \mathbf{x}_{t+1}, \mathcal{D}_t) = \mathbb{E}_g[\Phi(g(\mathbf{x}_{t+1})) | \mathcal{D}_t]$ , and  $\mu_{\mathcal{D}_t, \mathbf{x}_{t+1}, c_{t+1}}^*$  is the maximum of the posterior mean after observing  $(\mathcal{D}_t, \{\mathbf{x}_{t+1}, c_{t+1}\})$ . In supplementary B we show that the gradient of KG, required to maximize it efficiently, can be computed when using the Laplace approximation (see supplementary A) to approximate the GP posterior.

To extend the above KG acquisition function to contextual BBO, we simply add the context,  $\mathbf{s}$ , to the system parameters,  $\mathbf{x}$ , and replace  $g(\mathbf{x})$  with  $f(\mathbf{s}, \mathbf{x})$ . In this case, the maximization in Eqn 6 is performed only over the system parameters,  $\mathbf{x}$ , given a fixed context,  $\mathbf{s}_0$  (see supplementary C).

Computing the KG acquisition function is impractically slow for problems with moderately high dimensions, as its computation requires performing two nested optimizations: the optimization required for the Laplace approximation of the GP posterior (see supplementary C), and the maximization in Eqn 6. Thus, we looked for an alternative, that could scale to larger problems.

### 3.3 Sequential algorithm for choosing system parameters, $\mathbf{x}$ and context, $\mathbf{s}$

In our set-up, the parameters,  $\mathbf{x}$ , and  $\mathbf{s}$ , play two very different roles. The system parameters  $\mathbf{x}$  determine the system’s underlying performance,  $g(\mathbf{x})$ , which we want to maximize. The context,  $\mathbf{s}$ , determines how much information we gain about the system’s performance from binary observations,  $c$ . We therefore decided to choose  $\mathbf{x}$  and  $\mathbf{s}$  sequentially, using different heuristics: first,  $\mathbf{x}_{t+1}$  was chosen using binary BO, so as to optimize the system’s performance; next,  $\mathbf{s}_{t+1}$  was chosen using Bayesian active learning, to maximize the information we obtain from the binary observation,  $c_{t+1}$ .

#### 3.3.1 Choosing $\mathbf{x}$ using Bayesian optimization

We tested two different acquisition rules for selecting  $\mathbf{x}_{t+1}$ : GP Upper Credible Bound (GP-UCB) (Srinivas et al., 2010), and Thompson Sampling (TS) (Thompson, 1933).

Thompson sampling (TS) involves choosing  $\mathbf{x}_{t+1}$  by sampling from the distribution  $p(\mathbf{x}^* | \mathcal{D}_t)$ , where  $\mathbf{x}^*$  is defined, for a given objective function, as  $\mathbf{x}^* = \arg \max_{\mathbf{x}} f(\mathbf{x}, \mathbf{s})$  (note that, from Eqn 3,  $\mathbf{x}^*$  is independent of  $\mathbf{s}$ ). In supplementary section G we describe how to efficiently sample from  $p(\mathbf{x}^* | \mathcal{D}_t)$  in the context of GP classification and preference learning.

Second, we implemented a generalization of UCB to binary outputs, where  $\mathbf{x}_{t+1}$  is chosen by maximising the following acquisition function:

$$\alpha_{\text{UCB}}(\mathbf{x}) = \mathbb{E}(\Phi(f(\mathbf{x}, \mathbf{s})) + \beta \sqrt{\mathbb{V}(\Phi(f(\mathbf{x}, \mathbf{s})))}, \quad (8)$$

where a constant  $\beta$  (set to  $\beta = \Phi^{-1}(0.95)$ ) sets the balance between exploitation (first term on right hand side) and exploration (second term on right hand side). See Fauvel & Chalk (2021) for details on how to analytically compute this acquisition function and its gradient.

#### 3.3.2 Choosing $\mathbf{s}$ using Bayesian active learning

After choosing the system parameters,  $\mathbf{x}_{t+1}$ , the next step is to select a context  $\mathbf{s}_{t+1}$  such that the observation,  $c_{t+1}$  will be maximally informative about the underlying function  $f(\cdot, \mathbf{x}_{t+1})$ . To do this, we used the Bayesian Active Learning by Disagreement (BALD) algorithm, developed by Houlby et al. (2011).

For a given  $\mathbf{x}_{t+1}$ , the context  $\mathbf{s}_{n+1}$  is chosen so as to maximize the mutual information between the observation  $c_{t+1}$  and the objective function  $f(\cdot, \mathbf{x}_{t+1})$ ,  $I(c_{t+1}, f | \mathbf{s}_{t+1}, \mathbf{x}_{t+1})$ , which is given by:

$$I(c_{t+1}, f | \mathbf{s}_{t+1}, \mathbf{x}_{t+1}) = H(c_{t+1} | \mathbf{x}_{t+1}, \mathbf{s}_{n+1}) - \mathbb{E}_f[H(c_{t+1} | \mathbf{x}_{t+1}, \mathbf{s}_{n+1}, f)], \quad (9)$$

where  $H(c_{t+1} | \mathbf{x}_{t+1}, \mathbf{s}_{n+1})$  is the total entropy of  $c_{t+1}$ , and  $\mathbb{E}_f[H(c_{t+1} | \mathbf{x}_{t+1}, \mathbf{s}_{n+1}, f)]$  is the conditional entropy of  $c$ , given the latent function  $f(\cdot, \mathbf{x}_{t+1})$ . (Note that all three terms are also conditioned on the observed data,  $\mathcal{D}_t$ , which was removed from the equation for notational simplicity). This acquisition criterion can be efficiently approximated (Houlby et al., 2011).

### 3.4 Preferential Bayesian optimization

We next considered how to extend our method to preferential optimization (PBO). In standard PBO Brochu

et al. (2010); Gonzalez et al. (2017); Dewancker et al. (2017), i.e. with no contextual variable,  $\mathbf{s}$ , the result of an evaluation,  $c$ , depends on the relative value of the objective function,  $g$ , with two different parameter settings,  $\mathbf{x}$  and  $\mathbf{x}'$ , according to:

$$P(c = 1|g, \mathbf{x}, \mathbf{x}') = \Phi(g(\mathbf{x}) - g(\mathbf{x}')). \quad (10)$$

The parameters to be compared,  $\mathbf{x}$  and  $\mathbf{x}'$ , are called a duel. To extend this to the contextual case, we assume that the comparison depends on both the system parameters,  $\mathbf{x}$ , and context,  $\mathbf{s}$ , according to:

$$P(c = 1|f, \mathbf{s}, \mathbf{x}, \mathbf{x}') = \Phi(f(\mathbf{s}, \mathbf{x}) - f(\mathbf{s}, \mathbf{x}')), \quad (11)$$

where  $f(\mathbf{s}, \mathbf{x})$  is defined as before, such that, for all  $\mathbf{s} \in \mathcal{S}$ ,  $\arg \max_{\mathbf{x}} g(\mathbf{x}) = \arg \max_{\mathbf{x}} f(\mathbf{s}, \mathbf{x})$  (Eqn 3).

The generalization of the KG to this scenario is straightforward. Likewise, our sequential acquisition rule can be generalized to this scenario by selecting the duel  $(\mathbf{x}, \mathbf{x}')$  using PBO, and then choosing the context of the duel  $\mathbf{s}$  using Bayesian active learning.

In our experiments, we selected system parameters using either: (i) the KernelSelfSparring (KSS) algorithm (Sui & Burdick, 2017), which is a simple extension of TS, described above, or (ii) the Maximally Uncertain Challenge (MUC) acquisition rule, described in Fauvel & Chalk (2021). Contextual parameters,  $\mathbf{s}$ , were then selected using Bayesian active learning by disagreement (BALD; see previous section).

## 4 Experiments with synthetic test functions

To evaluate the performance of our method, we ran optimization experiments on a set of 34 functions from a widely used virtual library for optimization experiments (Surjanovic & Bingham, 2021). The functions in this library exhibit a diversity of behaviors that occur in real-life optimization problems.

For each objective function, we inferred the hyperparameters for three different kernels (squared exponential, Matérn 3/2 and Matérn 5/2) using maximum likelihood estimation with 1000 randomly chosen samples. We then determined for each function the kernel that best described the function by measuring the root-mean-squared error on 3000 points. The benchmark functions are listed in supplementary H. In all cases, we used the Laplace approximation to approximate the posterior over the objective,  $p(f|\mathcal{D})$ .

We introduced a scalar context variable  $s \in [0, 1]$ , so that for a test function  $g$  the response of a system query is 1 with probability  $P(s, \mathbf{x}) = \Phi(sg(\mathbf{x}))$  and 0 otherwise.

To take the context variable into account when building the GP surrogate model, we used the following kernel: for a base kernel  $k$  determined using the aforementioned procedure, we used:  $k_s((\mathbf{x}, s), (\mathbf{x}', s')) = ss'k(\mathbf{x}, \mathbf{x}')$ .

To compare the different algorithms, we used the stratified analysis method proposed by Dewancker et al. (2016). Briefly, for each benchmark function, we performed pairwise comparisons between acquisition functions using the Mann-Whitney U test at  $\alpha = 5 \times 10^{-4}$  significance on the best value found at the end of the optimization sequence. This determines a partial ranking based on the number of wins.

Ties are then broken by running the same procedure, but based on the Area Under Curve, which is related to the speed at which the algorithm reaches the optimum. This generates a new partial ranking, based on which a Borda score (Dwork et al., 2001) is attributed to each acquisition function (the Borda score of a candidate is the number of candidates with a lower rank). Then, rankings from different benchmarks are aggregated by summing the Borda scores to establish a global ranking. This can be seen as a weighted vote from each benchmark function.

### 4.1 Binary Bayesian optimization in adaptive contexts

We then ran optimizations on each function for 40 different random number generator seeds, on 60 iterations. The initial number of random samples was set to 5.

We termed the sequential acquisition rules in the binary feedback scenario TS with active learning by disagreement (TS-ALD) and GP-UCB with active learning by disagreement (UCB-ALD). We termed the generalization of KSS and MUC to the contextual scenario KSS-ALD and MUC-ALD.

We compared the different acquisition rules: the contextual binary knowledge gradient (cBKG), UCB-ALD and TS-ALD, with the following controls:

- Fully random, in which  $(s, \mathbf{x})$  was chosen at random at each iteration,
- $\mathbf{x}$  chosen using TS and  $s$  chosen randomly,
- $\mathbf{x}$  chosen using UCB and  $s$  chosen randomly,
- $(s, \mathbf{x})$  selected using BALD.

To avoid saturation effects when transforming the benchmark functions through the non-linearity, we scaled the functions so that they have mean 0 and variance 1. Examples of regret curves are presented in figure 1, and the results of the stratified analysis are summarized in table 1. More detailed results showing

pairwise comparisons between acquisition functions are presented in table S1.

UCB-ALD and TS-ALD show superior performance compared to cBKG (1), despite the fact that, compared to cBKG, where  $\mathbf{x}$  and  $\mathbf{s}$  are jointly selected, these sequential decision strategies induce an adaptivity gap (Jiang et al., 2019). Here, we used the Laplace approximation, given that Expectation Propagation (EP) is known to improve performance compared to the Laplace approximation and that the gradient of cBKG with EP seems intractable, this suggests that TS-ALD and UCB-ALD are better acquisition functions in general. The three heuristics outperformed the different controls.

Table 1: *Comparison of acquisition functions on benchmarks. UCB-ALD largely outperforms the other rules. Importantly, the sequential acquisition rules (TS-ALD and UCB-ALD) outperform cBKG.*

Acquisition rule	Rank	Borda score
UCB-ALD	1	144
TS-ALD	2	83
cBKG	3	59
UCB (random context)	4	46
BALD	5	35
TS (random context)	6	19
Random	7	10

## 4.2 Preferential Bayesian optimization in adaptive contexts

We then evaluated the performance of our sequential acquisition rules in their generalization to the case of preferential judgments: KSS-ALD and MUC-ALD. Given the limited performance of BKG in the previous experiments and the fact that the preferential version of Knowledge Gradient is impractically slow, we did not evaluate this acquisition function.

We then ran optimizations on each test function for 40 different random number generator seeds, on 60 iterations. We compared KSS-ALD and MUC-ALD to the following controls:

- Fully random, in which  $(s, \mathbf{x}_1, \mathbf{x}_2)$  was chosen at random at each iteration,
- $\mathbf{x}$  chosen using KSS and  $s$  chosen randomly,
- $\mathbf{x}$  chosen using MUC and  $s$  chosen randomly,
- $(s, \mathbf{x}_1, \mathbf{x}_2)$  selected using BALD.

Examples of regret curves are shown in figure 2, and the results of the stratified analysis are summarized in

figure 2. More detailed results showing pairwise comparisons between acquisition functions are presented in table S2. Again, adaptive selection of the context leads to superior performance compared to controls.

Table 2: *Comparison of acquisition functions on benchmarks. The sequential acquisition rules outperform the controls. MUC-ALD is the most efficient acquisition function.*

MUC-ALD	1	99
KSS-ALD	2	37
Kernel Self-Sparring	3	22
BALD	4	9
Random	5	5

## 5 Application: adaptive optimization in psychometric measurements

To illustrate the relevance of our algorithm, we considered the problem of optimizing the parameters of a lens to improve a patient’s vision based on their responses in a visual task.

Different types of visual defects typically result in different types of error (myopia results in ‘spherical refractive error’,  $S$ ; astigmatism results in ‘cylindrical refractive error’,  $C$ ). These errors induce image blur, but can be corrected by optimizing different optical parameters of a patient’s lenses. However, patients’ visual performance are typically assessed indirectly, for example by testing their performance in a visual task (e.g. asking patients to identify a letter, presented on-screen). Clearly, the task used to test patients’ visual performance will play a critical role in optimizing their vision. If the task is too easy/difficult (e.g. the letters presented onscreen are too small/large) then patients will always succeed/fail, and little information will be gained as to how to optimize their optics. In the following, we show our contextual BO algorithm can be used to address this problem.

### 5.1 Model of patients’ responses

A simple formula relates the spherico-cylindrical error (measured in diopters ( $\delta$ )) to image blur  $\beta$  (Raasch, 1995; Blendowske, 2015):

$$\beta = \sqrt{\frac{1}{2}(S^2 + (S + C)^2)} \quad (12)$$

We are thus trying to find the parameters of the optics  $\mathbf{x} = (S, C)$  that minimize  $\beta$ , or equivalently, minimize visual acuity (VA), defined as the log of the minimum angle of resolution (MAR, measured in minutes of

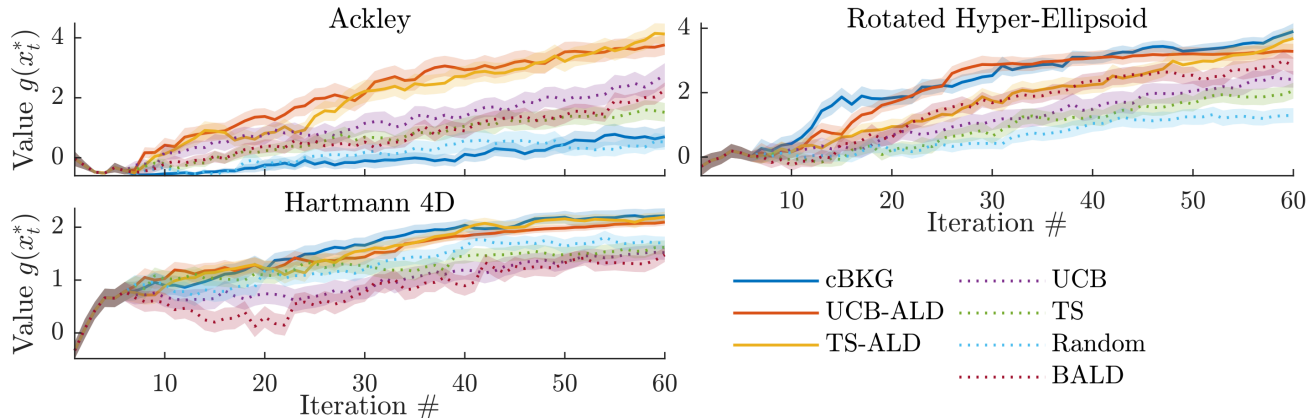


Figure 1: Results across three different objective functions and different methods in binary BO with adaptive contexts. Solid lines correspond to the mean value of the inferred maximum across the 40 repetitions. Shaded areas correspond to standard error on the mean. Either cBKG, UCB-ALD, or TS-ALD outperform the other acquisition rules, however, there is a lot of variability from one experiment to another. The cBKG acquisition rule tends to be less robust than the sequential heuristics.

arc). VA can be related to blur using the formula (Blendowske, 2015):

$$VA(\mathbf{x}) - VA(\mathbf{x}^*) = 1 + \beta^2,$$

where  $\mathbf{x}^*$  corresponds to the best correction. A VA of 20/20 corresponds to  $\log\text{MAR} = 0$ , so we considered that  $VA(\mathbf{x}^*) = 0$ .

We consider a simple model of subjects performing an  $n$ -alternatives forced-choice visual task, such as identifying a letter on a screen. The size of the letter,  $s$  (measured in log of the visual angle, in minutes of arc), determines the difficulty of this task. For a given optical correction  $\mathbf{x}$ , the probability of correct response is well described by a psychometric function (see e.g. Fülep et al. (2019) or Tokutake et al. (2011)):

$$P(c = 1|s) = \gamma + (1 - \gamma)\Phi(a(\mathbf{x})s + b(\mathbf{x})), \quad (13)$$

where  $\gamma$  is the chance probability of success,  $a$  and  $b$  are the slope and intercept of the psychometric curve.  $a$  is assumed to be strictly positive. Here, for simplicity and consistently with experimental evidence, we assumed that the slope of the psychometric function  $a(\mathbf{x})$  remains essentially constant with varying blur (Horner et al., 1985; Carkeet et al., 2001).

VA is usually defined as the value of  $s$  at which  $P(c = 1|s) = \frac{1+\gamma}{2}$ , or equivalently the inflexion point of the psychometric curve:  $VA(\mathbf{x}) = -\frac{b(\mathbf{x})}{a}$ .

To apply our algorithm to this problem, we define a function:

$$f(s, \mathbf{x}) = \Phi^{-1}[\gamma + (1 - \gamma)\Phi(as + b(\mathbf{x}))] \quad (14)$$

such that:  $P(c = 1|s, \mathbf{x}) = \Phi(f(s, \mathbf{x}))$  (as in Eqn 2). The problem of improving VA thus satisfies condition

3, as for any  $s$ , the maximum of  $f$  is the minimum of VA.

## 5.2 Gaussian process model

The use of GP classification for psychometric function estimation has been introduced by Gardner et al. (2015); Song et al. (2017, 2018) in the context of audiometry. We follow the same approach and build a GP model of the subject’s responses in the task.

For  $\gamma$  large enough, we have  $P(c = 1|s) \approx \Phi(a(\mathbf{x})s + b(\mathbf{x}))$ . Since in practice, with a letter chart,  $\gamma^{-1} = n = 26$ , we will make this simplifying assumption in building our surrogate model.

We put a GP prior on  $f$ , with zero mean and kernel  $k_\psi$  defined as:

$$k_\psi((s, \mathbf{x}), (s', \mathbf{x}')) = \theta ss' + k(\mathbf{x}, \mathbf{x}') \quad (15)$$

This kernel reflects the structure of the function  $f$  (see equation 14) with the assumption  $\gamma \approx 0$  (see supplementary E).

We used a squared exponential kernel as  $k$ . To minimize the effect of kernel hyperparameters, we simulated the response to 1000 random pairs  $(s, \mathbf{x})$  and inferred the kernel hyperparameters using maximum likelihood estimation. The hyperparameters were then kept constant during the experiments.

## 5.3 Results

We repeated the simulated experiment 20 times for 260 iterations, for 8 different slopes values (evenly spaced between between  $1.0 \log\text{MAR}^{-1}$  and  $8.0 \log\text{MAR}^{-1}$ ).

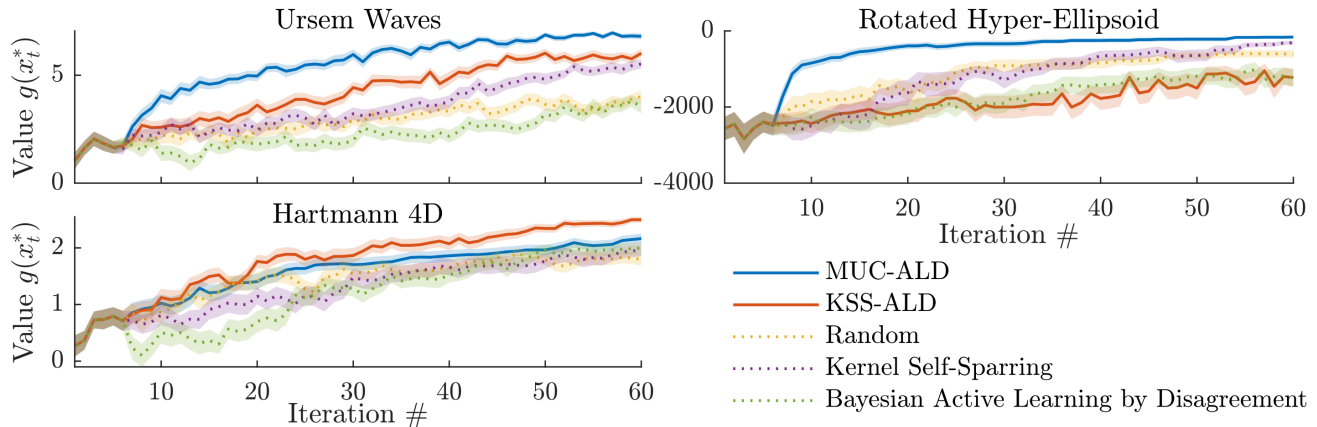


Figure 2: Results across three different objective functions in preferential BO with adaptive contexts. Solid lines correspond to the mean value of the inferred maximum across the 40 repetitions. Shaded areas correspond to standard error on the mean. Sequential acquisition rules (KSS-ALD and MUC-ALD) consistently outperform the others.

The search space was  $\mathcal{X} = [-4\delta, 4\delta] \times [-4\delta, 4\delta]$  and the context space  $\mathcal{S} = [-1, 2] \log\text{MAR}$ . Regret curves in the experiments where the slope of the psychometric function was set at  $5.0 \log\text{MAR}^{-1}$  are shown on figure 3, and the results of the stratified analysis are summarized in table 3.

Both UCB-ALD and TS-ALD led to rapid and consistent improvement of the VA closed to its optimal value of  $\log\text{MAR} = 0$ . UCB-ALD is the best performing algorithm (see table 3), with a mean VA at the end of the optimization sequence of  $2.48 \times 10^{-2} \log\text{MAR}$  in the case of a slope of  $5.0 \log\text{MAR}^{-1}$  (s.e.m. = 8.22), 3). At the end of the optimization sequence, the an average spherical correction error of  $2.74 \times 10^{-2}\delta$  (s.e.m. =  $5.36 \times 10^{-2}$ ). Note that this is closed to the precision that can be achieved nowadays ( $0.01\delta$ ). The average cylindrical correction error is  $1.53 \times 10^{-1}\delta$  (s.e.m. =  $8.22 \times 10^{-2}$ ).

However, when using random sampling, the optimization consistently failed (figure 3). Overall, the results are consistent with the one obtained on the synthetic benchmarks (table 3).

Here, we considered that the objective is a black box. However, for a specific application in a clinical setting, parameterizing the objective using domain knowledge would likely lead to faster and more robust improvement (see e.g. Cox & De Vries (2017)).

## 6 Discussion

### 6.1 Summary of contributions

In this paper, we introduced a new framework for binary and preferential BO: BO in adaptive contexts, in

Table 3: Comparison of acquisition functions on the refractive error correction experiment with 8 different slopes (evenly spaced between between  $1.0 \log\text{MAR}^{-1}$  and  $8.0 \log\text{MAR}^{-1}$ ). The two heuristics combining BO and active learning (UCB-ALD and TS-ALD) outperform the controls where the context (TS, UCB, random) or the correction (BALD, random) are not adaptively selected.

Acquisition rule	Rank	Borda score
UCB-ALD	1	35
TS-ALD	2	26
UCB (random context)	3	15
BALD	4	8
TS (random context)	5	3
Random	6	0

which the experimenter can choose the context where each function evaluation is performed. We proposed an acquisition function to jointly select the optimization variable and the context and showed how to generalize existing acquisition functions to this framework by combining them with Bayesian active learning. We show on synthetic benchmarks that the proposed algorithms outperform controls in which the context is not adaptively selected, in both BOs with binary or preference feedbacks. Finally, we showcase our framework on a concrete problem: tuning the parameters of the lens for patients with refractive errors.

### 6.2 Related work

In the bandit setting, contextual GP bandit (Krause & Ong, 2011) extends the GP bandit framework to



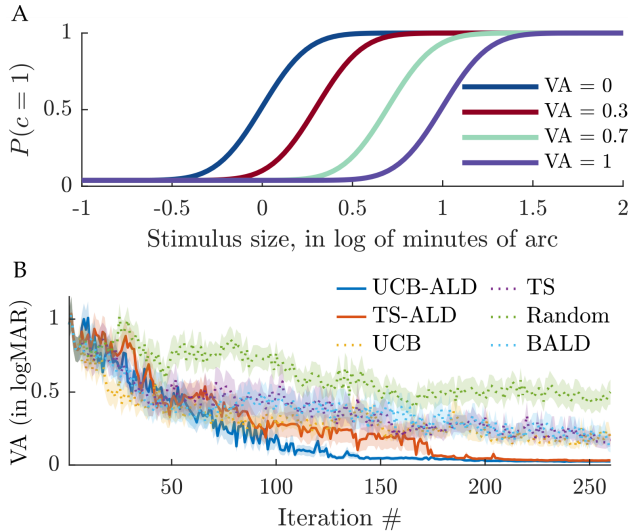


Figure 3: **A.** Psychometric curves for various refractive errors corresponding to different visual acuities, with a slope of the psychometric function set at  $5.0 \log\text{MAR}^{-1}$ . The baseline corresponds to the chance level in the  $n$ -alternatives forced-choice task (here,  $n = 26$ ). VA of 20/20 corresponds to  $\log\text{MAR} = 0$ . **B.** Visual acuity with the inferred best parameters throughout the optimization. The lines correspond to the average over 60 repetitions, whereas the shaded areas correspond to standard error on the mean. UCB-ALD and TS-ALD both lead to faster convergence towards optimal correction ( $\log\text{MAR} = 0$ ) compared to controls where the context (TS, UCB, random) or the correction (BALD, random) are not adaptively selected.

scenarios in which at each round corresponds a given random context, and actions are taken knowing this context. The goal is to identify the best arm averaged over all possible contexts. This framework has been generalized to dueling bandits (Dudík et al., 2015). Our work differs as we consider the problem of both selecting a context and action at each iteration.

The methods most related to our work are BO with expensive integrands (Toscano-Palmerin & Frazier, 2018), conditional BO (Pearce et al., 2020), and contextual policy search (Pinsler et al., 2019), where the goal is to maximize the expected performance conditionally on a random context variable. During the optimization process, this context variable is controlled by the experimenter. In BO with expensive integrands (Toscano-Palmerin & Frazier, 2018), the goal is to maximize a function averaged over a set of random conditions, when function evaluation is noise-free or with i.i.d. Gaussian noise. The authors used a generalization of the knowledge gradient. Pearce et al. (2020) further generalized by considering the case where function evaluations are performed in parallel and batch of inputs are selected

at each iteration. Our work is a generalization to the binary and preferential feedback scenarios, which implies new challenges. Indeed, even when the objective function is the same across different contexts, the amount of information we get from each evaluation varies with the context in a way that is a priori unknown. This problem arises in general when the amount of noise in function evaluation varies with the context, but we only considered the case of probit likelihoods for simplicity. We also introduced sequential acquisition rules that allow the generalization of acquisition rules used in BO. We did not consider whether sequential acquisition also improves performance in the case of Gaussian likelihood, and this should be the topic of future work. In this paper, we considered the case where the optimum of the function  $f$  is the same across all contexts. In general, the maximum of  $f(\mathbf{s}, \cdot)$  may depend on  $\mathbf{s}$ . In that case, several criteria may be considered. Either we may want to maximize the averaged performance of the system across contexts, or we may want to maximize the worst-case performance of the device. We let the study of these generalizations for future work.

### 6.3 Code availability

Matlab implementation available at [https://disclose\\_upon\\_release](https://disclose_upon_release).

### References

- Antonova, R., Rai, A., and Atkeson, C. G. Deep Kernels for Optimizing Locomotion Controllers. In *ICML*, jul 2017.
- Bishop, C. M. *Pattern Recognition and Machine Learning*. Springer, 2006.
- Blendowske, R. Unaided Visual Acuity and Blur. *Optom. Vis. Sci.*, 92(6):e121–e125, 2015.
- Brochu, E., Brochu, T., and Freitas, N. A Bayesian interactive optimization approach to procedural animation design. *Comput. Animat. 2010 - ACM SIGGRAPH / Eurographics Symp. Proceedings, SCA 2010*, pp. 103–112, 2010.
- Calandriello, D., Carratino, L., Lazaric, A., Valko, M., and Rosasco, L. Gaussian Process Optimization with Adaptive Sketching: Scalable and No Regret. In *Proc. Mach. Learn. Res.*, volume 99, pp. 1–25, mar 2019.
- Carkeet, A., Lee, L., Kerr, J. R., and Keung, M. M. The slope of the psychometric function for Bailey-Lovie letter charts: Defocus effects and implications for modeling letter-by-letter scores. *Optom. Vis. Sci.*, 78(2):113–121, 2001.



- Cox, M. and De Vries, B. A parametric approach to Bayesian optimization with pairwise comparisons. In *Nips*, 2017.
- Dewancker, I., McCourt, M., Clark, S., Hayes, P., Johnson, A., and Ke, G. A Stratified Analysis of Bayesian Optimization Methods. *arXiv*, 2016.
- Dewancker, I., Bauer, J., and McCourt, M. Sequential Preference-Based Optimization. *arXiv*, 2017.
- Dudík, M., Hofmann, K., Schapire, R. E., Slivkins, A., and Zoghi, M. Contextual dueling bandits. *J. Mach. Learn. Res.*, 40(2015):1–25, 2015.
- Dwork, C., Kumar, R., Naor, M., and Sivakumar, D. Rank aggregation methods for the web. *Proc. 10th Int. Conf. World Wide Web, WWW 2001*, pp. 613–622, 2001.
- Fauvel, T. and Chalk, M. Efficient exploration in binary and preferential Bayesian optimization. *arXiv*, 2021.
- Frazier, P., Powell, W., and Dayanik, S. The knowledge-gradient policy for correlated normal beliefs. *INFORMS J. Comput.*, 21(4):599–613, 2009.
- Fülep, C., Kovács, I., Kránitz, K., and Erdei, G. Simulation of visual acuity by personalizable neurophysiological model of the human eye. *Sci. Rep.*, 9(1):1–15, 2019.
- Gardner, J. R., Weinberger, K. Q., Malkomes, G., Barbour, D., Garnett, R., and Cunningham, J. P. Bayesian active model selection with an application to automated audiometry. *Adv. Neural Inf. Process. Syst.*, 2015-Janua:2386–2394, 2015.
- Gonzalez, J., Dai, Z., Damianou, A., and Lawrence, N. D. Preferential Bayesian optimization. *34th Int. Conf. Mach. Learn. ICML 2017*, 3:2080–2089, 2017.
- Grado, L. L., Johnson, M. D., and Netoff, T. I. Bayesian adaptive dual control of deep brain stimulation in a computational model of Parkinson’s disease. *PLoS Comput. Biol.*, 14(12):1–23, 2018.
- Hernández-Lobato, J. M., Hoffman, M. W., and Ghahramani, Z. Predictive entropy search for efficient global optimization of black-box functions. *Adv. Neural Inf. Process. Syst.*, 1(January):918–926, 2014.
- Horner, D. G., Paul, A. D., Katz, B., and Bedell, H. E. Variations in the Slope of the Psychometric Acuity Function with Acuity Threshold and Scale. *Optom. Vis. Sci.*, 62(12):895–900, dec 1985.
- Houlsby, N., Huszár, F., Ghahramani, Z., and Lengyel, M. Bayesian Active Learning for Classification and Preference Learning. *arXiv*, pp. 1–17, dec 2011.
- Jiang, S., Chai, H., Gonzalez, J., and Garnett, R. BINOCULARS for Efficient, Nonmyopic Sequential Experimental Design. *arXiv*, 1(8):2–4, sep 2019.
- Krause, A. and Ong, C. S. Contextual Gaussian process bandit optimization. *Adv. Neural Inf. Process. Syst. 24 25th Annu. Conf. Neural Inf. Process. Syst. 2011, NIPS 2011*, pp. 1–9, 2011.
- Lázaro-Gredilla, M., Quiñonero-Candela, J., Rasmussen, C. E., and Figueiras-Vidal, A. R. Sparse spectrum gaussian process regression. *J. Mach. Learn. Res.*, 11:1865–1881, 2010.
- Milgrom, P. and Segal, I. Envelope theorems for arbitrary choice sets. *Econometrica*, 70(2):583–601, 2002.
- Minka, T. P. *A family of algorithms for approximate Bayesian inference*. PhD thesis, Massachusetts Institute of Technology, 2001.
- Mutný, M. and Krause, A. Efficient high dimensional Bayesian optimization with additivity and quadrature fourier features. *Adv. Neural Inf. Process. Syst.*, 2018-Decem(NeurIPS):9005–9016, 2018.
- Nielsen, J., Nielsen, J., and Larsen, J. Perception-based Personalization of Hearing Aids using Gaussian Processes and Active Learning. *IEEE/ACM Trans. Audio, Speech, Lang. Process.*, 23(1):1–1, 2014.
- Pearce, M., Klaise, J., and Groves, M. ConBO: Conditional Bayesian Optimization. *arXiv*, 2020.
- Pinsler, R., Karkus, P., Kupcsik, A., Hsu, D., and Lee, W. S. Factored Contextual Policy Search with Bayesian Optimization. *arXiv*, pp. 7242–7248, apr 2019.
- Raasch, T. W. Spherocylindrical refractive errors and visual acuity. *Optom. Vis. Sci.*, 72(4):272–275, 1995.
- Rasmussen, C. E. and Williams, K. I. *Gaussian Processes for Machine Learning*. The MIT Press, 2006.
- Riutort-Mayol, G., Burkner, P. C., Andersen, M. R., Solin, A., and Vehtari, A. Practical hilbert space approximate bayesian gaussian processes for probabilistic programming. *arXiv*, pp. 1–33, 2020.
- Seeger, M. Notes on Minka’s expectation propagation for Gaussian process classification, 2002.
- Snoek, J., Larochelle, H., and Adams, R. P. Practical Bayesian Optimization of Machine Learning Algorithms. In *Proc. 25th Int. Conf. Neural Inf. Process. Syst.*, volume 2, pp. 2951–2959, jun 2012.

- Solin, A. and Särkkä, S. Hilbert space methods for reduced-rank Gaussian process regression. *Stat. Comput.*, 30(2):419–446, 2020.
- Song, X. D., Garnett, R., and Barbour, D. L. Psychometric function estimation by probabilistic classification. *J. Acoust. Soc. Am.*, 141(4):2513–2525, 2017.
- Song, X. D., Sukesan, K. A., and Barbour, D. L. Bayesian active probabilistic classification for psychometric field estimation. *Attention, Perception, Psychophys.*, 80(3):798–812, 2018.
- Srinivas, N., Krause, A., Kakade, S., and Seeger, M. Gaussian process optimization in the bandit setting: No regret and experimental design. *ICML 2010 - Proceedings, 27th Int. Conf. Mach. Learn.*, pp. 1015–1022, 2010.
- Sui, Y. and Burdick, J. W. Correlational dueling bandits with application to clinical treatment in large decision spaces. *IJCAI Int. Jt. Conf. Artif. Intell.*, pp. 2793–2799, 2017.
- Surjanovic, S. and Bingham, D. Virtual Library of Simulation Experiments: Test Functions and Datasets. Retrieved July 29, 2021, from <http://www.sfu.ca/~ssurjano>, 2021.
- Tesch, M., Schneider, J., and Choset, H. Expensive function optimization with stochastic binary outcomes. *30th Int. Conf. Mach. Learn. ICML 2013*, 28:2320–2328, 2013.
- Thompson, W. R. On the Likelihood that One Unknown Probability Exceeds Another in View of the Evidence of Two Samples. *Biometrika*, 25(3/4):285, dec 1933.
- Tokutake, T., Mita, N., Kawamoto, K.-I., Kani, K., and Tabuchi, A. Relation between Visual Acuity and Slope of Psychometric Function in Young Adults. *Iperception.*, 2(4):308–308, 2011.
- Toscano-Palmerin, S. and Frazier, P. I. Bayesian Optimization with Expensive Integrands. *arXiv*, pp. 1–52, mar 2018.
- Wang, Z., Gehring, C., Kohli, P., and Jegelka, S. Batched Large-scale Bayesian Optimization in High-dimensional Spaces. *Int. Conf. Artif. Intell. Stat. AISTATS 2018*, 84:745–754, jun 2017.
- Wilson, J. T., Borovitskiy, V., Terenin, A., Mostowsky, P., and Deisenroth, M. P. Efficiently Sampling Functions from Gaussian Process Posteriors. *arXiv*, 2020a.
- Wilson, J. T., Borovitskiy, V., Terenin, A., Mostowsky, P., and Deisenroth, M. P. Pathwise conditioning of gaussian processes. *arXiv*, 2020b.
- Wu, J. and Frazier, P. I. The parallel knowledge gradient method for batch Bayesian optimization. *Adv. Neural Inf. Process. Syst.*, 2016.
- Zhang, Y., Dai, Z., and Low, B. K. H. Bayesian optimization with binary auxiliary information. *35th Conf. Uncertain. Artif. Intell. UAI 2019*, 2019.

## Contextual Bayesian optimization with binary outputs: Supplementary Materials

---

### A The Laplace approximation for Gaussian process classification

The following description of Laplace approximation for Gaussian process classification is given for completeness. It is required in order to understand the computation of the gradient of the Binary Knowledge Gradient. We follow the reasoning presented in Rasmussen & Williams (2006) as well as Bishop (2006), to which we refer the reader for further details.

In Gaussian process classification, we assume that observations  $\mathbf{c}$  at points  $\mathbf{X} = [\mathbf{x}_1, \dots, \mathbf{x}_t]$  are Bernoulli random variables with parameters  $\mu_c(\mathbf{X}) = \pi(f(\mathbf{X}))$ , where  $f$  is a latent function, and  $\pi$  is an inverse link function. We choose the convention where  $c$  is either 0 or 1.

The predictive distribution at point  $\mathbf{x}$  is given by:

$$p(c = 1|\mathbf{x}, \mathcal{D}) = \int p(c = 1|f(\mathbf{x}))p(f(\mathbf{x})|\mathcal{D})df(\mathbf{x}). \quad (\text{S1})$$

Since this integral is analytically intractable, we approximate  $p(f(\mathbf{x})|\mathcal{D})$  with a Gaussian distribution. Indeed, for a a random normally distributed random variable  $z$ :

$$\int \Phi(z)\mathcal{N}(z|\mu, \sigma^2)dz = \Phi\left(\frac{\mu}{\sqrt{1 + \sigma^2}}\right). \quad (\text{S2})$$

A convenient way to do so is to note that:

$$p(f(\mathbf{x})|\mathcal{D}) = \int p(f(\mathbf{x})|\mathbf{f})p(\mathbf{f}|\mathcal{D})d\mathbf{f}, \quad (\text{S3})$$

where  $\mathbf{f}$  is the vector of latent values at training points  $X$ . From the formula for Gaussian process posteriors, we have:

$$p(f(\mathbf{x})|\mathbf{f}) = \mathcal{N}\left(f(\mathbf{x})|\mathbf{k}^\top \mathbf{K}^{-1} \mathbf{f}, k(\mathbf{x}, \mathbf{x}) - \mathbf{k}^\top \mathbf{K}^{-1} \mathbf{k}\right), \quad (\text{S4})$$

where  $\mathbf{K} = k(\mathbf{X}, \mathbf{X})$  and  $\mathbf{k} = k(\mathbf{X}, \mathbf{x})$ .

The second term in the integral  $p(\mathbf{f}|\mathcal{D})$  is the posterior distribution of the latent value function at training points. By approximating it with a Gaussian distribution, then we could compute the integral in S3, which would give us a Gaussian approximation for  $p(f(\mathbf{x})|\mathcal{D})$ . This approximation would in turn allow us to compute S1.

#### A.1 Principle of the Laplace approximation

We start by finding a Gaussian approximation of  $p(\mathbf{f}|\mathcal{D})$ . In general, for a random variable  $\mathbf{z}$  whose probability density function is  $p(\mathbf{z}) = \frac{f(\mathbf{z})}{Z}$ , we can use a second order Taylor expansion around the mode  $\mathbf{z}_0$  of the distribution (where the gradient vanishes) so that:

$$\ln f(\mathbf{z}) \sim \ln f(\mathbf{z}_0) - \frac{1}{2}(\mathbf{z} - \mathbf{z}_0)^\top \mathbf{H}(\mathbf{z} - \mathbf{z}_0), \quad (\text{S5})$$

where  $\mathbf{H}$  is the negative of the Hessian of  $f$  at  $\mathbf{z}_0$ .

Taking the exponential and computing the appropriate normalization coefficients, we have:

$$p(\mathbf{z}) \sim \frac{|\mathbf{H}|^{\frac{1}{2}}}{(2\pi)^{\frac{D}{2}}} \exp\left(-\frac{1}{2}(\mathbf{z} - \mathbf{z}_0)^\top \mathbf{H}(\mathbf{z} - \mathbf{z}_0)\right) = \mathcal{N}(\mathbf{z}|\mathbf{z}_0, \mathbf{H}^{-1}) \quad (\text{S6})$$

This method of approximating a probability density function with a Gaussian probability density function is called the Laplace approximation.

## A.2 Gaussian approximation of the posterior

In order to find a Gaussian approximation of  $p(\mathbf{f}|\mathcal{D})$ , we thus need to compute its mode and its Hessian. By using Bayes' rule, we have:

$$\ln p(\mathbf{f}|\mathcal{D}) = \ln p(\mathbf{f}) + \ln p(\mathcal{D}|\mathbf{f}). \quad (\text{S7})$$

The prior term is:

$$\ln p(\mathbf{f}) = -\frac{1}{2}\mathbf{f}^\top \mathbf{K}^{-1}\mathbf{f} - \frac{t}{2}\ln(2\pi) - \frac{1}{2}\ln|\mathbf{K}|. \quad (\text{S8})$$

The likelihood term is:

$$\begin{aligned} \ln p(\mathcal{D}|\mathbf{f}) &= \ln \left( \prod_{i=1}^t \pi(f_i)^{c_i} (1 - \pi(f_i))^{(1-c_i)} \right) \\ &= \sum_{i=1}^t \ln \left( \pi(f_i)^{c_i} (1 - \pi(f_i))^{(1-c_i)} \right). \end{aligned} \quad (\text{S9})$$

So the gradient of the the log-posterior is:

$$\nabla_{\mathbf{f}} \ln p(\mathbf{f}|\mathcal{D}) = \nabla_{\mathbf{f}} \ln p(\mathcal{D}|\mathbf{f}) - \mathbf{K}^{-1}\mathbf{f}, \quad (\text{S10})$$

whereas the Hessian is:

$$\nabla_{\mathbf{f}}^2 \ln p(\mathbf{f}|\mathcal{D}) = \nabla_{\mathbf{f}}^2 \ln p(\mathcal{D}|\mathbf{f}) - \mathbf{K}^{-1}, \quad (\text{S11})$$

where  $\nabla^2$  refers to the Hessian matrix.

We introduce  $\mathbf{W} = -\nabla_{\mathbf{f}}^2 \ln p(\mathcal{D}|\mathbf{f})$ , which is a diagonal matrix since conditionally on  $\mathbf{f}$ , observations are independent.

$$\frac{\partial \ln p(c_i|f_i)}{\partial f_i} = \frac{\pi'(f_i)(c_i - \pi(f_i))}{\pi(f_i)(1 - \pi(f_i))}. \quad (\text{S12})$$

In the case where the link function is the cumulative normal distribution:

$$\frac{\partial \ln p(c_i|f_i)}{\partial f_i} = \frac{(2c_i - 1)\phi(f_i)}{\Phi((2c_i - 1)f_i)}, \quad (\text{S13})$$

and

$$\frac{\partial^2 \ln p(c_i|f_i)}{\partial f_i^2} = -\frac{\phi(f_i)^2}{\Phi((2c_i - 1)f_i)^2} - \frac{(2c_i - 1)f_i\phi(f_i)}{\Phi((2c_i - 1)f_i)}. \quad (\text{S14})$$

The mode  $\mathbf{f}_0$  satisfies the condition  $\nabla_{\mathbf{f}} \ln p(\mathbf{f}|\mathcal{D}) = 0$ , so  $\mathbf{f}_0 = \mathbf{K}\nabla_{\mathbf{f}} \ln p(\mathcal{D}|\mathbf{f})$ . The mode is usually found using the Newton-Raphson method.

The approximate posterior distribution is :

$$p(\mathbf{f}|\mathcal{D}) = \mathcal{N}(\mathbf{f}_0, (\mathbf{K}^{-1} + \mathbf{W})^{-1}). \quad (\text{S15})$$

## A.3 Approximate predictive distribution

By combining equation with equation S15, we get:

$$\mathbb{E}_{\mathbf{f}}[f(\mathbf{x})|\mathcal{D}] = \mathbf{k}^\top \mathbf{K}^{-1}\mathbf{f}_0, \quad (\text{S16})$$

and:

$$\nabla_{\mathbf{f}}[f(\mathbf{x})|\mathcal{D}] = k(\mathbf{x}, \mathbf{x}) - \mathbf{k}^\top (\mathbf{K} + \mathbf{W}^{-1})^{-1}\mathbf{k}. \quad (\text{S17})$$

## B Gradient of the knowledge gradient

The knowledge gradient is defined as:

$$\text{KG}(\mathbf{x}) = \mathbb{E}_{c \sim p(c|\mathcal{D})}(\mu_{n+1}^* - \mu_n^* | \mathcal{D}, \mathbf{x}_{n+1} = \mathbf{x}), \quad (\text{S18})$$

where  $\mu_{n+1}^*$  is the maximum of the posterior mean after observing  $(\mathcal{D}, (\mathbf{x}, c))$ , and  $\mu_n^*$  is the maximum of the posterior mean after observing  $\mathcal{D} = (\mathbf{X}, c_{1 \dots n})$ .

With binary outputs, the knowledge gradient can be expressed as:

$$\text{KG}(\mathbf{x}) = \mu_c(\mathbf{x})(\mu_{1,n+1}^* - \mu_n^*) + (1 - \mu_c(\mathbf{x}))(\mu_{0,n+1}^* - \mu_n^*), \quad (\text{S19})$$

where  $\mu_c(\mathbf{x}) = \mathbb{E}_f[\Phi(f(\mathbf{x})) | \mathcal{D}]$ , and  $\mu_{1,n+1}^*$  (resp.  $\mu_{0,n+1}^*$ ) is the maximum of the posterior mean after observing  $(\mathcal{D}, (\mathbf{x}, 1))$  (resp.  $(\mathcal{D}, (\mathbf{x}, 0))$ ). That is:

$$\mu_{c,n+1}^* = \max_{\mathbf{x}' \in \mathcal{X}} \mathbb{E}_f[f(\mathbf{x}') | \mathcal{D} \cup (\mathbf{x}, c)]. \quad (\text{S20})$$

The gradient of the knowledge-gradient is given by:

$$\nabla \text{KG}(\mathbf{x}) = \nabla \mu_c(\mathbf{x})(\mu_{1,n+1}^* - \mu_{0,n+1}^*) + \mu_c(\mathbf{x}) \nabla \mu_{1,n+1}^* + (1 - \mu_c(\mathbf{x})) \nabla \mu_{0,n+1}^*. \quad (\text{S21})$$

To compute the gradients of  $\mu_{1,n+1}^*$  and  $\mu_{0,n+1}^*$ , inspired by Wu & Frazier (2016), we use the envelope theorem (Milgrom & Segal, 2002), which states that, under sufficient regularity conditions, the gradient with respect to  $\mathbf{x}$  of a maximum of a collection of functions of  $\mathbf{x}$  is given simply by first finding the maximum  $\mathbf{x}^*$  in this collection, and then differentiating this single function with respect to  $\mathbf{x}$ , keeping  $\mathbf{x}^*$  fixed. Here, we have an infinite collection of functions  $\mathbb{E}_f[f(\mathbf{x}') | \mathcal{D} \cup (\mathbf{x}, c)]$  indexed by  $\mathbf{x}'$ .

**Theorem 1.** *Corollary 4 of the envelope theorem in Milgrom & Segal (2002) Let  $X$  denote the choice set and  $t$  be a parameter in a  $[0, 1]$  (the theorem generalizes to normed vector spaces). Let  $f : X \times [0, 1] \rightarrow \mathbb{R}$  be an objective function parameterized by  $t$ . We define:*

$$V(t) = \sup_{\mathbf{x} \in \mathcal{X}} f(\mathbf{x}, t), \quad (\text{S22})$$

$$X^*(t) = \{\mathbf{x} \in \mathcal{X}, f(\mathbf{x}, t) = V(t)\}. \quad (\text{S23})$$

Suppose that  $X$  is a nonempty compact space,  $f(\mathbf{x}, t)$  is upper semicontinuous in  $\mathbf{x}$ , and  $\frac{\partial f}{\partial t}(\mathbf{x}, t)$  is continuous in  $(\mathbf{x}, t)$ . Then:

$$\forall t \in [0, 1], V'(t+) = \max_{\mathbf{x} \in X^*(t)} \frac{\partial f}{\partial t}(\mathbf{x}, t), \quad (\text{S24})$$

$$\forall t \in (0, 1], V'(t-) = \min_{\mathbf{x} \in X^*(t)} \frac{\partial f}{\partial t}(\mathbf{x}, t). \quad (\text{S25})$$

$V$  is differentiable at any  $t \in (0, 1)$  if and only if  $\left\{ \frac{\partial f}{\partial t}(\mathbf{x}, t) | \mathbf{x} \in X^*(t) \right\}$  is a singleton, and in that case  $\forall \mathbf{x} \in X^*(t), V'(t) = \frac{\partial f}{\partial t}(\mathbf{x}, t)$ .

As a consequence, by writing  $\mathbf{x}^* = \arg \max_{\mathbf{x}' \in \mathcal{X}} \mathbb{E}_f[f(\mathbf{x}') | \mathcal{D} \cup (\mathbf{x}, c)]$ , we get:

$$\nabla_x \mu_{c,n+1}^* = \nabla_x \mathbb{E}_f[f(\mathbf{x}^*) | \mathcal{D} \cup (\mathbf{x}, c)]. \quad (\text{S26})$$

From the Laplace approximation, we have:

$$\mathbb{E}_f[f(\mathbf{x}^*) | \mathcal{D} \cup (\mathbf{x}, c)] = \mathbf{k}^\top \nabla_{\mathbf{y}} \log p(\mathbf{c} | \mathbf{y}), \quad (\text{S27})$$

where  $\mathbf{y}$  corresponds to the inferred latent values of the training data,  $\mathbf{c} = c_{1 \dots n+1}$ , and  $\mathbf{k} = k((\mathbf{X}, \mathbf{x}), \mathbf{x}^*)$ .

So that:

$$\begin{aligned}
 \nabla_{\mathbf{x}} \mathbb{E}[f(\mathbf{x}^*) | \mathcal{D} \cup (\mathbf{x}, c)] &= (\nabla_{\mathbf{x}} \mathbf{k}^\top) \nabla_{\mathbf{y}} \log p(\mathbf{c} | \mathbf{y}) + \mathbf{k}^\top \nabla_{\mathbf{x}} \nabla_{\mathbf{y}} \log p(\mathbf{c} | \mathbf{y}) \\
 &= (\nabla_{\mathbf{x}} \mathbf{k}^\top) \nabla_{\mathbf{y}} \log p(\mathbf{c} | \mathbf{y}) + \mathbf{k}^\top (\nabla_{\mathbf{y}}^2 \log p(\mathbf{c} | \mathbf{y})) \nabla_{\mathbf{x}} \mathbf{y} \\
 &= (\nabla_{\mathbf{x}} \mathbf{k}^\top) \nabla_{\mathbf{y}} \log p(\mathbf{c} | \mathbf{y}) - \mathbf{k}^\top \mathbf{W} \nabla_{\mathbf{x}} \mathbf{y},
 \end{aligned} \tag{S28}$$

where  $\mathbf{W} = -\nabla_{\mathbf{y}}^2 \log p(\mathbf{c} | \mathbf{y})$ .

From the Laplace approximation, we have  $\mathbf{y} = \mathbf{K} \nabla_{\mathbf{y}} \log p(\mathbf{c} | \mathbf{y})$ , where  $\mathbf{K} = k((\mathbf{X}, \mathbf{x}), (\mathbf{X}, \mathbf{x}))$ .

By differentiating this self-consistent equation,

$$\begin{aligned}
 \nabla_{\mathbf{x}} \mathbf{y} &= (\nabla_{\mathbf{x}} \mathbf{K}) \nabla_{\mathbf{y}} \log p(\mathbf{c} | \mathbf{y}) + \mathbf{K} (\nabla_{\mathbf{y}}^2 \log p(\mathbf{c} | \mathbf{y})) \nabla_{\mathbf{x}} \mathbf{y} \\
 &= (\nabla_{\mathbf{x}} \mathbf{K}) \nabla_{\mathbf{y}} \log p(\mathbf{c} | \mathbf{y}) - \mathbf{K} \mathbf{W} \nabla_{\mathbf{x}} \mathbf{y}.
 \end{aligned} \tag{S29}$$

By rearranging:

$$\nabla_{\mathbf{x}} \mathbf{y} = (\mathbf{I} + \mathbf{K} \mathbf{W})^{-1} \nabla_{\mathbf{x}} \mathbf{K} \nabla_{\mathbf{y}} \log p(\mathbf{c} | \mathbf{y}). \tag{S30}$$

## C Contextual binary knowledge gradient

With binary outputs and contexts, the knowledge gradient can be expressed as:

$$\text{KG}(\mathbf{s}, \mathbf{x}) = \mu_c(\mathbf{s}, \mathbf{x}) \mu_{t+1,1}^* + (1 - \mu_c(\mathbf{s}, \mathbf{x})) \mu_{t+1,0}^* - \mu_t^*, \tag{S31}$$

where  $\mu_c(\mathbf{s}, \mathbf{x}) = P(c = 1 | \mathbf{s}, \mathbf{x}, \mathcal{D}_t) = \mathbb{E}_f[\Phi(f(\mathbf{s}, \mathbf{x})) | \mathcal{D}_t]$  is the predictive class distribution, and  $\mu_{t+1,1}^*$  (resp.  $\mu_{t+1,0}^*$ ) is the maximum of the posterior mean for an arbitrary context  $\mathbf{s}_0$  after observing  $(\mathcal{D}_t \cup (\mathbf{x}, 1))$  (resp.  $(\mathcal{D}_t \cup (\mathbf{x}, 0))$ ). That is:

$$\mu_{t+1,c}^* = \max_{\mathbf{x}' \in \mathcal{X}} \mathbb{E}_f[f(\mathbf{s}_0, \mathbf{x}') | \mathcal{D}_t \cup (\mathbf{s}_0, \mathbf{x}, c)]. \tag{S32}$$

Note that the term  $\mu_t^*$  in Eqn S31 can be neglected, since it does not depend on  $(\mathbf{s}, \mathbf{x})$ .

Importantly, if the kernel reflects the assumption that the maximum of the objective  $f$  does not depend on the context  $\mathbf{s}$ , then  $\mu_{t+1,c}^*$  can be computed for an arbitrary value of  $\mathbf{s}_0$ . Indeed, following the Laplace approximation (supplementary A), with latent values  $\mathbf{f}_0$ :

$$\mathbb{E}_f[f(\mathbf{s}, \mathbf{x}) | \mathcal{D}] = \mathbf{k}((\mathbf{s}, \mathbf{x}), (S, X))^\top \mathbf{K}^{-1} \mathbf{f}_0, \tag{S33}$$

where  $(S, X)$  corresponds to training points. Consider for example the case where  $f(\mathbf{s}, \mathbf{x}) = h(\mathbf{s})g(\mathbf{x})$ , the kernel reflecting this structure is of the form  $k((\mathbf{s}, \mathbf{x}), (\mathbf{s}', \mathbf{x}')) = k_h(\mathbf{s}, \mathbf{s}')k_g(\mathbf{x}, \mathbf{x}')$ . In that case, the posterior mean factorizes and it is clear that we can take the maximum with respect to  $\mathbf{x}$  independently of  $\mathbf{s}$ .

## D Supplementary results

<b>A</b>							
Random	0.03	0.00	0.00	0.03	0.06	0.00	0.00
TS	0.00	0.00	0.03	0.03	0.06	0.00	0.06
BALD	0.06	0.00	0.09	0.06	0.00	0.03	0.12
UCB	0.00	0.00	0.06	0.00	0.12	0.06	0.24
cBKG	0.03	0.00	0.00	0.15	0.15	0.15	0.18
TS-ALD	0.03	0.00	0.09	0.09	0.29	0.12	0.32
UCB-ALD	0.00	0.12	0.24	0.03	0.32	0.44	0.50

<b>B</b>							
Random	0.00	0.00	0.03	0.00	0.09	0.00	0.00
TS	0.00	0.00	0.06	0.00	0.06	0.00	0.06
BALD	0.00	0.00	0.12	0.06	0.00	0.09	0.15
UCB	0.00	0.00	0.09	0.00	0.06	0.09	0.15
cBKG	0.03	0.00	0.00	0.06	0.21	0.12	0.09
TS-ALD	0.00	0.00	0.12	0.03	0.26	0.09	0.29
UCB-ALD	0.00	0.24	0.38	0.09	0.65	0.47	0.71

UCB-ALD    TS-ALD    cBKG    UCB    BALD    TS    Random

Figure S1: Detailed results of performance comparison between acquisition functions in contextual Binary Bayesian optimization. Each entry  $(i,j)$  corresponds to the fraction of benchmarks functions for which  $i$  beats  $j$  according to the Mann-Whitney  $U$  test at  $\alpha = 5 \times 10^{-4}$  significance based either on the best value found (**A**) or the Area Under the Curve (**B**).



**A**

Random	0.06	0.00	0.00	0.03	0.00
BALD	0.09	0.00	0.00	0.00	0.06
KSS	0.09	0.03	0.00	0.15	0.24
KSS-ALD	0.09	0.00	0.06	0.21	0.26
MUC-ALD	0.00	0.47	0.44	0.53	0.59

**B**

Random	0.00	0.00	0.00	0.03	0.00
BALD	0.00	0.00	0.00	0.00	0.03
KSS	0.00	0.00	0.00	0.12	0.12
KSS-ALD	0.06	0.00	0.06	0.24	0.24
MUC-ALD	0.00	0.50	0.53	0.56	0.74

MUC-ALD      KSS-ALD      KSS      BALD      Random

Figure S2: Detailed results of performance comparison between acquisition functions in contextual Preferential Bayesian optimization. Each entry  $(i,j)$  corresponds to the fraction of benchmarks functions for which  $i$  beats  $j$  according to the Mann-Whitney  $U$  test at  $\alpha = 5 \times 10^{-4}$  significance based either on the best value found (**A**) or the Area Under the Curve (**B**).

## E Kernel derivation for the psychophysics experiment

For lens parameters,  $\mathbf{x}$ , the response of the patient is determined by:

$$P(c = 1 | s, \mathbf{x}) = \gamma + (1 - \gamma)\Phi(a(\mathbf{x})s + b(\mathbf{x})). \quad (\text{S34})$$

For  $\gamma$  large enough, we have  $P(c = 1 | s) \approx \Phi(a(\mathbf{x})s + b(\mathbf{x}))$ . Since in practice, with a letter chart,  $\gamma^{-1} = n = 26$ , we will make this simplifying assumption in building our surrogate model.

We put a GP prior on  $f$ , with zero mean and kernel  $k_\psi$  defined as:

$$k_\psi((s, \mathbf{x}), (s', \mathbf{x}')) = \theta ss' + k(\mathbf{x}, \mathbf{x}') \quad (\text{S35})$$

This kernel reflects the structure of the function  $f$  (see equation 14) with the assumption  $\gamma \approx 0$ . Indeed, we have:

$$\begin{aligned} \text{Cov}(f(s, \mathbf{x}), f(s', \mathbf{x}')) &= \text{Cov}(a(\mathbf{x})s + b(\mathbf{x}), a(\mathbf{x}')s' + b(\mathbf{x}')) \\ &= ss' \text{Cov}(a(\mathbf{x})s + b(\mathbf{x}), a(\mathbf{x}')s' + b(\mathbf{x}')) \\ &\quad + (s + s') \text{Cov}(a(\mathbf{x}), b(\mathbf{x}')) + \text{Cov}(b(\mathbf{x}), b(\mathbf{x}')) \end{aligned} \quad (\text{S36})$$

We put GP priors on functions  $a$  and  $b$ , with kernels  $k_1$  and  $k_2$  respectively. since  $a(\mathbf{x})$  and  $b(\mathbf{x})$  are a priori independent conditionally on  $\mathbf{x}$ , the second term on the right-hand side vanishes, so that:

$$\text{Cov}(f(s, \mathbf{x}), f(s', \mathbf{x}')) = ss'k_1(\mathbf{x}, \mathbf{x}') + k_2(\mathbf{x}, \mathbf{x}') \quad (\text{S37})$$

Since we assumed the slope to be constant at value  $\sqrt{\theta}$ , this further simplifies to:

$$\text{Cov}(f(s, \mathbf{x}), f(s', \mathbf{x}')) = \theta ss' + k(\mathbf{x}, \mathbf{x}') \quad (\text{S38})$$

## F Visual acuity as a function of the correction parameters

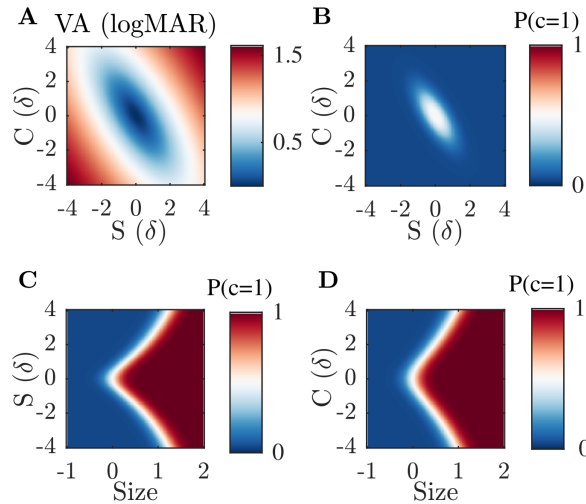


Figure S3: **A.** Visual acuity as a function of the correction parameters  $S$  (spherical correction) and  $C$  (cylindrical correction) in diopters ( $\delta$ ). The slope of the psychometric curve is kept fixed at  $5.0 \log\text{MAR}^{-1}$ . **B.** Probability of correct response in a 26-alternatives forced choice task for a stimulus of visual angle  $1'$ . In blue regions, the subject will always perform at chance level, independently of the correction parameters, so responses will be uninformative.

## G Sampling from GP classification models

Acquisition rules based on Thompson sampling rely on samples from the posterior distribution over the maximum:

$$p(\mathbf{x}^* | \mathcal{D}) = p\left(f(\mathbf{x}^*) = \max_{\mathbf{x} \in \mathcal{X}} f(\mathbf{x}) | \mathcal{D}\right) \quad (\text{S39})$$

Hernández-Lobato et al. (2014) proposed the following sampling scheme: draw a sample from the posterior distribution  $p(f|\mathcal{D})$ , then return the maximum of the sample. One could iteratively construct the sample  $f$  while it is being optimized but, as noted by Hernández-Lobato et al. (2014), this would have a cost  $\mathcal{O}(m^3)$ , where  $m$  is the number of evaluations of the function necessary to find the maximum. Although this is doable in practice, Hernández-Lobato et al. (2014) suggested a more efficient procedure by sampling a finite-dimensional approximation to  $f$ , based on a finite-dimensional approximation to the kernel  $k(\mathbf{x}, \mathbf{x}') \sim \phi(\mathbf{x})^\top \phi(\mathbf{x}')$  (Lázaro-Gredilla et al., 2010). In GP classification and preference learning, this approximate sampling cannot be directly applied. In the following section, we will explain how to apply existing approximate sampling methods to the case of GP classification models.

### G.1 Kernel approximation

The sampling methods mentioned above consists in approximating a stationary kernel  $k$  by means of the inner product of features  $\phi$  such that:  $k(\mathbf{x}, \mathbf{x}') \sim \phi(\mathbf{x})^\top \phi(\mathbf{x}')$ . Recently, a method was proposed by Solin & Särkkä (2020), which aims at making the approximation as good as possible for a given rank (see Riutort-Mayol et al. (2020) for details about the practical implementation). In this method, the kernel is approximated using a series expansion in terms of eigenfunctions of the Laplace operator on a rectangular domain  $\Omega = [-L_1, L_1] \times \dots \times [-L_d, L_d]$  (the search space is usually rectangular in Bayesian optimization).

In preference learning, a specific difficulty arises. Indeed, the base kernel used to model the value function may be shift-invariant, the preference kernel, however, is not in general. This inexact hypothesis introduced in the sampling algorithm, leads to samples that are not consistent with the anti-symmetric property of a preference function, i.e.  $f(\mathbf{x}, \mathbf{x}') = -f(\mathbf{x}', \mathbf{x})$ , (see e.g. figure 4.1 in Gonzalez et al. (2017) where this inexact stationarity hypothesis is introduced).

However, assume that we have a finite dimensional approximation to the base kernel  $k(\mathbf{x}, \mathbf{x}') \sim \phi(\mathbf{x})^\top \phi(\mathbf{x}')$ , it is easy to see that we can approximate the preference kernel by  $k_{\text{pref}}((\mathbf{x}_i, \mathbf{x}_j), (\mathbf{x}_k, \mathbf{x}_l)) \sim \phi_{\text{pref}}(\mathbf{x}_i, \mathbf{x}_j)^\top \phi_{\text{pref}}(\mathbf{x}_k, \mathbf{x}_l)$ , with:

$$\phi_{\text{pref}}(\mathbf{x}_i, \mathbf{x}_j) = \phi(\mathbf{x}_i) - \phi(\mathbf{x}_j) \quad (\text{S40})$$

By construction, the corresponding sample is anti-symmetric.

### G.2 Weight-space approximation with non-Gaussian likelihoods

The most widely used method for approximate sampling from GP in Bayesian optimization is the weight-space approximation. Assume that we have a finite-dimensional approximation to the kernel  $k(\mathbf{x}, \mathbf{x}') \sim \phi(\mathbf{x})^\top \phi(\mathbf{x}')$ . The features  $\phi(\mathbf{x})$  can be used to approximate the Gaussian process posterior with a Bayesian linear model:  $f(\mathbf{x}) \sim \phi(\mathbf{x})^\top \boldsymbol{\omega}$ , where (Lázaro-Gredilla et al., 2010):

$$\boldsymbol{\omega} \sim \mathcal{N}\left((\Phi^\top \Phi + \sigma^2 I)^{-1} \Phi^\top \mathbf{y}, (\Phi^\top \Phi + \sigma^2 I)^{-1} \sigma^2\right) \quad (\text{S41})$$

In the case of non-Gaussian likelihoods, , naively replacing  $\mathbf{y}$  in S41 by the latent values inferred by the Laplace approximation (see A) or Expectation Propagation would not take into account the correlated heteroscedastic noise on the latent function values at training points. To the extent of our knowledge, the process of weight-space approximate sampling has not been rigorously introduced for latent GP models. Here, we suggest to use a sampling process in two steps. First, samples  $\mathbf{y}$  are drawn from the posterior distribution over the latent variables at training points:  $\mathcal{N}(\boldsymbol{\mu}, \boldsymbol{\Sigma})$ , then  $\boldsymbol{\omega}$  is sampled from  $\boldsymbol{\omega} \sim \mathcal{N}\left((\Phi^\top \Phi + \sigma^2 I)^{-1} \Phi^\top \mathbf{y}, (\Phi^\top \Phi + \sigma^2 I)^{-1} \sigma^2\right)$ , where  $\sigma$  is a small constant used for regularization.

To see why this sampling scheme is correct, note that:  $p(f(\mathbf{x})|\mathcal{D}) = \int p(f(\mathbf{x})|X, \mathbf{y})p(\mathbf{y}|\mathcal{D})d\mathbf{y}$ . So given latent values sampled from  $p(\mathbf{y}|\mathcal{D})$ , an approximate sample  $\tilde{f}$  can be drawn from  $p(f(\mathbf{x})|X, \mathbf{y})$  using the method of Hernández-Lobato et al. (2014).

However, the degeneracy, i.e., low-rankness of the GP approximation, causes the estimate to grow over-confident when the number of observed points exceeds the degrees of freedom of the approximation. This results in ill-behaved approximations, and, in particular, underestimated variance, in regions far away from the data points. This phenomenon is known as variance starvation (Wang et al., 2017; Mutný & Krause, 2018; Calandriello et al., 2019).

### G.3 Decoupled-bases approximate sampling

Recently Wilson et al. (2020a) proposed an efficient way to sample from GP posteriors that avoids variance starvation. The original sampling method was devised for exact GP with Gaussian noise and sparse GP, where the GP is computed based on a set of inducing points that explain the data, however, it can easily be generalized to non-Gaussian likelihood with a latent function (Wilson et al., 2020b).

Briefly, this method is based on a corollary of Matheron’s rule. For a Gaussian process  $f \sim \mathcal{GP}(0, k)$ , the latent process conditioned on latent values  $(X, \mathbf{y})$  admits, in distribution, the representation:

$$\underbrace{(f | \mathbf{y})(\cdot)}_{\text{posterior}} \stackrel{d}{=} \underbrace{f(\cdot)}_{\text{prior}} + \underbrace{k(\cdot, \mathbf{x}) \mathbf{K}^{-1}(\mathbf{y} - f(X))}_{\text{update}} \quad (\text{S42})$$

This corollary defines an approximation to the Gaussian process conditioned on  $(X, \mathbf{y})$ , where the stationary prior is approximated with a Bayesian linear model (weight-space prior), and the approximate posterior is obtained by adding an exact update (function-space update):

$$\underbrace{(f | \mathbf{y})(\cdot)}_{\text{posterior}} \stackrel{d}{\approx} \underbrace{\sum_{i=1}^{\ell} \omega_i \phi_i(\cdot)}_{\text{weight-space prior}} + \underbrace{\sum_{j=1}^m v_j k(\cdot, \mathbf{x}_j)}_{\text{function space update}} \quad , \quad (\text{S43})$$

where  $\mathbf{v} = \mathbf{K}^{-1}(\mathbf{y} - \Phi\boldsymbol{\omega})$ , and  $\boldsymbol{\omega}$  is sampled from  $\mathcal{N}(\mathbf{0}, I)$ . This method is termed decoupled-bases decomposition of the GP.

To sample from the posterior latent function, we thus sample  $\boldsymbol{\omega}$  from  $\mathcal{N}(\mathbf{0}, I)$  and compute the corresponding weight-space prior, then sample  $\mathbf{y}$  from  $\mathcal{N}(\mu_f(X), \Sigma_f(X, X))$  and compute the corresponding function-space update.

## H Benchmarks

Name	D	Kernel	Space
Ackley	2	Matérn 3/2	$[-32.768, 32.768]^2$
Beale	2	SE-ARD	$[-4.5, 4.5]^2$
Bohachevsky	2	SE-ARD	$[-100, 100]^2$
Three-Hump Camel	2	Matérn 5/2	$[-5, 5]^2$
Six-Hump Camel	2	SE-ARD	$[-3, 3] \times [-2, 2]$
Colville	4	Matérn 5/2	$[-10, 10]^4$
Cross-in-Tray	2	Matérn 5/2	$[-10, 10]^2$
Dixon-Price	2	Matérn 5/2	$[-5, 5]^2$
Drop-Wave	2	Matérn 3/2	$[-5.12, 5.12]^2$
Eggholder	2	SE-ARD	$[-512, 512]^2$
Forrester et al (2008)	1	SE-ARD	$[0, 1]$
Goldstein-Price	2	SE-ARD	$[-2, 2]^2$
Griewank	2	SE-ARD	$[-600, 600]^2$
Gramacy and Lee (2012)	1	SE-ARD	$[0.5, 2.5]$
Hartmann 3-D	3	SE-ARD	$[0, 1]^3$
Hartmann 4D	4	SE-ARD	$[0, 1]^4$
Hartmann 6D	6	SE-ARD	$[0, 1]^6$
Holder	2	SE-ARD	$[-10, 10]^2$
Langer	2	Matérn 3/2	$[0, 10]^2$
Levy	2	SE-ARD	$[-10, 10]^2$
Levy N.13	2	Matérn 5/2	$[-10, 10]^2$
Perm 0,d, $\beta$	2	SE-ARD	$[-2, 2]^2$
Perm d, $\beta$	2	SE-ARD	$[-2, 2]^2$
Powell	4	SE-ARD	$[-4, 5]^4$
Rosenbrock	2	SE-ARD	$[-2.048, 2.048]^2$
Rotated Hyper-Ellipsoid	2	Matérn 3/2	$[-65.536, 65.536]^2$
Schaffer n4	2	Matérn 3/2	$[-100, 100]^2$
Schwefel	2	SE-ARD	$[-500, 500]^2$
Shekel	4	SE-ARD	$[0, 10]^4$
Schubert	2	Matérn 3/2	$[0, 10]^2$
Sphere	2	SE-ARD	$[-5.12, 5.12]^2$
Sum Squares	2	SE-ARD	$[-10, 10]^2$
Trid	2	SE-ARD	$[-4, 4]^2$
Ursem Waves	2	SE-ARD	$[-1.2, 1.2] \times [-0.9, 1.2]$

Table S1: *Benchmark functions in Bayesian optimization experiments.*